The Mechanism of Spontaneous Oscillatory Contractions in Skeletal Muscle

D. A. Smith and D. G. Stephenson*
Department of Zoology, La Trobe University, Melbourne, Victoria 3086, Australia

ABSTRACT Most striated muscles generate steady contractile tension when activated, but some preparations, notably cardiac myocytes and slow-twitch fibers, may show spontaneous oscillatory contractions (SPOC) at low levels of activation. We have provided what we believe is new evidence that SPOC is a property of the contractile system at low actin-myosin affinity, whether caused by a thin-filament regulatory system or by other means. We present a quantitative single-sarcomere model for isotonic SPOC in skeletal muscle with three basic ingredients: i), actin and myosin filaments initially in partial overlap, ii), stretch activation by length-dependent changes in the lattice spacing, and iii), viscoelastic passive tension. Modeling examples are given for slow-twitch and fast-twitch fibers, with periods of 10 s and 4 s respectively. Isotonic SPOC occurs in a narrow domain of parameter values, with small minimum and maximum values for actin-myosin affinity, a minimum amount of passive tension, and a maximum transient response rate that explains why SPOC is favored in slow–twitch fibers. The model also predicts the contractile, relaxed and SPOC phases as a function of phosphate and ADP levels. The single-sarcomere model can also be applied to a whole fiber under auxotonic and fixed-end conditions if the remaining sarcomeres are treated as a viscoelastic load. Here the model predicts an upper limit for the load stiffness that leads to SPOC; this limit lies above the equivalent loads expected from the rest of the fiber.

INTRODUCTION

Spontaneous oscillatory contraction, or ''SPOC'', in striated muscle and muscle fibers is not a new phenomenon. It was first observed by Fabiato and Fabiato (1) in cardiac muscle and by Stephenson and Williams (2,3) in skeletal muscle (rat soleus), in both cases at low levels of activation by calcium (pCa $\equiv -\log_{10}[Ca^{2+}] > 6$). When the ends of the fiber were fixed, the observed oscillations in fiber tension were accompanied by nonuniform oscillatory changes in the lengths of short segments of the fiber, showing a characteristic wave-like motion (4). In skeletal muscle, SPOC is observed commonly in slow fibers, with a period of 3–10 s at room temperature; in fast fibers SPOC has been observed in a very narrow range of calcium levels (5), with periods of 1–2 s. In skeletal muscle, SPOC is observed only in a range of sarcomere lengths where the thick and thin filaments are not in complete overlap (3,5), which at high activation generates the descending limb of the tension-length curve (6,7).

Early observations of SPOC were confined to submicromolar Ca^{2+} levels, suggesting that the phenomenon was a property of the thin-filament Ca^{2+}-regulatory system as well as the contractile apparatus. At low calcium, isometric tension can increase with sarcomere length on the descending limb because of increased contractile activation at longer lengths, the so-called stretch activation effect (3,8). We did propose a model of SPOC based on sarcomere-length-dependent changes in Ca^{2+}-sensitivity of the regulatory system, in which the time delay was responsible for the SPOC period (9). However, the equilibration times for tropomyosin movements, and troponin-I movements between actin and TnC, are both under 2 ms (10,11), which is much too fast to account for the period of oscillations, typically ~5 s in slow fibers. Moreover, more recent experiments show that thin-filament Ca^{2+}-regulation is not a necessary ingredient of the mechanism of SPOC. Ishiwata et al. (12) have shown that SPOC could be induced in the absence of Ca^{2+} by adding mM ADP. Similarly, we have observed SPOC in skinned rat soleus fibers in the absence of Ca^{2+} by using low ionic strength to raise actomyosin affinity to the required level (Fig. 1). Conversely, Ishiwata and colleagues observed spontaneous oscillatory contractions in cardiac muscle fibers with added inorganic phosphate (Pi) (13) and in reconstituted fibers with no regulatory proteins, when actin-myosin interactions were inhibited by the addition of 20 mM 2,3-butanedione monoxime (14). Thus SPOC must be an intrinsic property of the contractile system when actin-myosin binding is reduced, either in the presence of the troponin-tropomyosin regulatory system at low calcium, or in other ways.

Starting from these insights, we have constructed what we believe is a new model in which SPOC in skeletal muscle is predicted by the contractile system at low levels of activation, whether by low $[Ca^{2+}]$ or changes in ionic strength, 2,3-butanedione monoxime, ADP, or Pi. The key ingredients of the model are i), sarcomeres with partially overlapping filaments where the number of myosins interacting with F-actin decreases linearly with sarcomere length, ii), stretch activation as a property of the contractile system, and iii), passive tension displaying viscoelastic properties as shown in Fig. 2 *A*. Stretch activation as a property of the contractile system can be generated by a decrease in lattice spacing with increasing length (15–17) and hence a thermally activated increase in actin-myosin affinity and binding rate, as shown

Submitted November 19, 2008, and accepted for publication January 23, 2009.

*Correspondence: George.Stephenson@latrobe.edu.au

Editor: Shin'ichi Ishiwata.

0006-3495/09/05/3682/10 $2.00

doi: 10.1016/j.bpj.2009.01.039

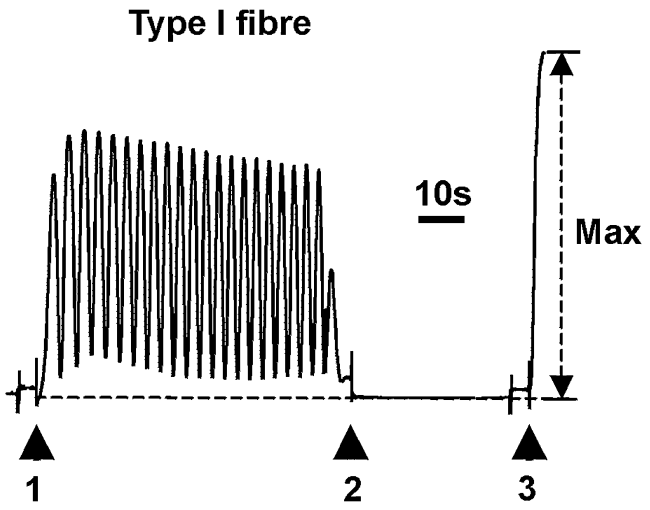

FIGURE 1 Representative isometric force responses from a mechanically skinned type I (slow-twitch) soleus muscle fiber of the rat (average sarcomere length 2.8 μm) at 25°C and [Ca^{2+}] < 10 nM when transferred from a standard ionic strength ($\Gamma/2 = 225$ mM) relaxing solution used in our laboratory (2) ([Ca^{2+}] < 10 nM) to a low ionic-strength relaxing solution ($\Gamma/2 =$ 61 mM; [Ca^{2+}] < 10 nM; EGTA, 12.5 mM; ATP, 2 mM; [Mg^{2+}], 0.75 mM; creatine phosphate, 2.5 mM; HEPES, 22.5 mM; [Na^{+}], 9 mM; [K^{+}], 32 mM; pH = 7.10) at the time indicated by arrow 1. At arrow 2, the fiber was transferred back to the standard ionic strength relaxing solution and at arrow 3, the fiber was transferred to the low ionic strength, maximally Ca^{2+}-activating solution with 12.5 mM Ca-EGTA ([Ca^{2+}] ~30 μM). The dotted lines below traces indicate the zero force level.

recently in the presence of mM ADP (18). Activation by Ca^{2+} can then be described entirely in terms of its effects on actin-myosin interactions. With regulated F-actin, the strength of these interactions increase with the free Ca^{2+} concentration, but the thin-filament regulatory system as such is not part of the model. The passive tension component displays hysteresis when measured at increasing and decreasing lengths due to unwinding/unfolding and rewinding/refolding of the titin molecules that connect myosin filaments to the Z-lines (19,20). This property is mimicked by assuming that passive tension is linearly viscoelastic.

The most ordered form of SPOC, in which all sarcomeres oscillate in synchrony, has been observed in a single myofibril under isotonic conditions (21), which suggests that a single-sarcomere model at constant force is a reasonable starting point for modeling. Its dynamics can be characterized by just two functions of time, namely myosin-generated tension $T_M(t)$ for a fixed number of myosins in overlap, and sarcomere length $L(t)$. The model also requires passive tension as a function of sarcomere length and velocity, and the fraction of myosins in overlap as a function of length; both these functions are well characterized experimentally.

Under isotonic conditions, this model works as follows. When a muscle is activated and then held at a constant load F, there is a corresponding half-sarcomere length $L_o(F)$ at partial overlap for which this force is exactly balanced by the sum of active and passive tensions in the half-sarcomere (Fig. 3 *A*); this length defines a fixed point of the system, namely a steady state that is maintained if nothing is disturbed. This fixed point can be stable or unstable to small perturbations.

1. At high levels of activation, there can be three fixed points for a given load because the net isometric tension $T_0(L)$ at partial filament overlap is a decreasing function of L (Fig. 3 *A*). The fixed points on the ascending limb and near zero overlap are stable, because the slopes of the $T_0(L)$ curve at these points are positive and therefore, displacements from the fixed point generate a restoring force. However, the fixed point on the descending limb

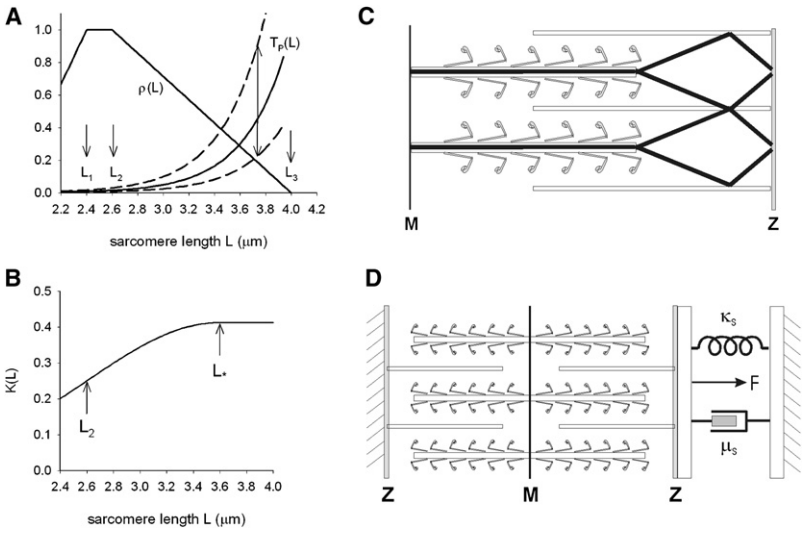

FIGURE 2 Elements of a single-sarcomere model for SPOC. (*A*) Isometric properties against sarcomere length L. The fraction $\rho(L)$ of actin and myosin filaments in overlap as a function of sarcomere length, showing the ascending limb, a plateau at full overlap between L_1 and L_2, and the descending limb out to zero overlap at length L_3 (6,7). At full activation, the net myosin tension is proportional to overlap. Passive tension is an exponentially increasing function (Eq. 1), depending on the velocity of length change (*up* and *down arrows* indicate +ve and −ve velocities). (*B*) Myosin affinity for actin , $K(L)$ is assumed to increase with sarcomere length (Eq. 5) because the lattice spacing decreases, until myosins span the lateral spacing between myosin and actin filaments at a length L_*. (*C*) The titin-based mechanism of Cazorla et al. (15) for stretch activation. If slack titin filaments (16), shown in black, bind to the surrounding F-actins near the Z-line, radial forces develop at longer sarcomere lengths that will decrease the lattice spacing d. This decrease is observed in both cardiac and skeletal muscles (15,17) and is approximately linear in L with slope γ, permitting stronger myosin-actin binding if the myosin rod bends under thermal activation. Thus $K(L) = K_*\exp(-\kappa_{rod}(d - d_*)^2/2k_BT)$ (k_B = Boltzmann constant, T = absolute temperature) is the myosin affinity for $d > d_*$, where $L < L_*$. Hence $\Delta = \kappa_{rod}\gamma^2/k_BT$ in Eq. 5 of the main text. (*D*) A cartoon of the single sarcomere coupled to an auxotonic load, defined by an elastic element of stiffness κ_S and a dashpot with damping constant μ_S.

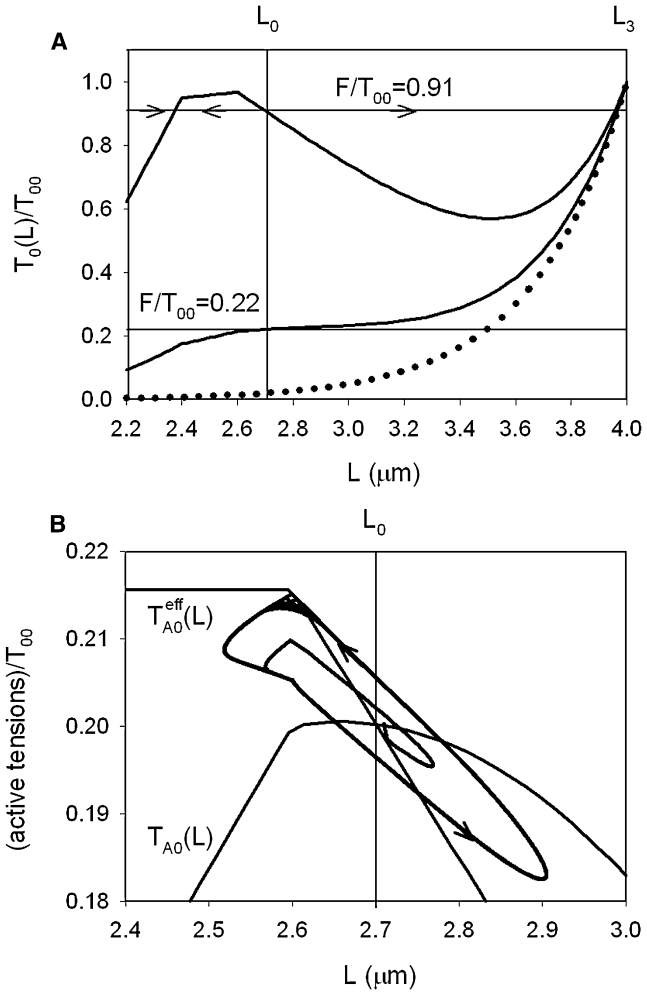

FIGURE 3 The mechanisms for popping and SPOC behavior under isotonic conditions. (*A*) Net isometric tension $T_0(L)$ as a fraction of maximally activated plateau tension T_{00} versus sarcomere length L, at high and low levels of activation ($K_2 = 20$ and 0.25). In each case there is a constant load F ($0.91T_{00}$ and $0.22T_{00}$) that intersects the tension curve at the same length $L_0 = 2.7$ μm on the descending limb; this intersection is a fixed point of the system. For the upper curve, the slope at this fixed point is negative and the system is unstable as indicated by the arrows. For the lower curve, the slope is positive but the stability of the fixed point remains in question if stretch activation contributes to the rise in tension beyond L_0. (*B*) At the lower level of activation, SPOC can occur because stretch activation only contributes to active tension after a time delay to give the active component $T_{A0}(L) = \rho(L)T_{M0}(L)$ of isometric tension. Starting at L_0, the active component of isometric tension before myosins detach kinetically and rebind is $T_{A0}^{eff}(L) = \rho(L)T_{M0}(L_0)$, which decreases with L. As a function of time, the active tension $T_A(t)$ attempts to move between these curves, and the heavy curve is a phase-plane plot produced by the model. Equal and opposite changes in passive tension $T_P(L(t))$ (not shown) are required to maintain the isotonic condition.

is unstable; any small increase in length will magnify the drop in force, causing the sarcomere to pop out to the stable fixed point at the longer sarcomere length (22). Similarly, a small decrease in length will cause the sarcomere to shorten to the fixed point on the ascending limb.

2. At very small levels of activation, there is only one fixed point, which is stable because passive tension predominates and passive tension is an exponentially increasing function of sarcomere length (15,23).
3. In between, there is a range of activation levels in which net isometric tension increases with sarcomere length L in the region of partial overlap, but active tension is present (Fig. 3 *A*). As L increases above the fixed point L_0, isometric active tension would follow the overlap fraction down to small values if bound myosins detached from actin only when they moved out of overlap (the lower curve of Fig. 3 *B*). However, some myosins in the overlap zone will detach by binding ATP, and in the presence of stretch activation they will rebind more strongly at the new length. The sarcomere would then attempt to move toward the true steady-state active tension at the current length (the upper curve of Fig. 3 *B*); there is an instability generated by the time delay from myosin cycling before stretch activation at the new length can take effect. This instability will generate maintained length oscillations (SPOC) if net isometric tension rises above the load at longer lengths; this can happen solely because of stretch activation, or from stretch activation in conjunction with viscoelastic passive tension.

Under isotonic conditions and in the absence of inertial forces, the constant force supplied at the ends of the fiber is transmitted equally to all sarcomeres, whose lengths should oscillate in phase unless structural inhomogeneities are present. SPOC has also been observed under auxotonic conditions, where there is a damped elastic load (24). Here the sarcomeres do not oscillate strictly in phase and a wavefront propagates repeatedly down the fiber. In these circumstances, a multisarcomeric model is required, but the single-sarcomere model should still be qualitatively correct for one sarcomere if the remainder of the fiber is approximated by a spring and dashpot in parallel. Then the model shows that SPOC can occur under a wide range of auxotonic boundary conditions such as might arise from the rest of the fiber. This approach should also predict SPOC in fixed-end fibers, observed as periodic oscillations in fiber tension.

The Model

For a single sarcomere with length $L(t)$ at time t, the net tension $T(t)$ in the cross-section of the fiber can be written as

$$T(t) = \rho(t)T_M(t) + T_P(L(t))(1 + \mu_P v(t)), \qquad (1)$$

where the subscripts M and P refer to active and passive components respectively, and $v(t) = dL/dt$ is the velocity of lengthening. Here $\rho(t)$ is the fraction of myosin heads in overlap with actin filaments, so $T_M(t)$ is active tension after the number of myosins in overlap has been scaled up to the total number present. It is assumed to satisfy the rate equation

$$\dot{T}_M(t) = -r(L(t))\{T_M(t) - T_{M0}(L(t))\psi(v(t))\}, \quad (2)$$

which provides a single-rate description of the slowest (phase-4) tension response to length changes (25). Here $T_{M0}(L)$ is the scaled isometric tension at length L, and

$$\psi(v) = 1 + \frac{\alpha v}{1 + \beta_{\pm}|v|} \quad (3)$$

is a suitable multiplier for steady-state tension as a function of v. For $v < 0$, this function is equivalent to Hill's equation $(T_M + a)|v| = b(T_{M0} - T_M)$, with $\alpha \equiv b^{-1}(1 + a/T_{M0})$ and $\beta_- \equiv 1/b$ (26). For $v > 0$, a different value of β_+ can be used to generate a suitable tension-velocity curve for steady lengthening (27). For passive tension, the isometric tension $T_P(L)$ can be represented by the exponential function $T_{P0}\exp(\xi(L - L_3))$ where L_3 is the length for zero overlap (Fig. 2 *A*). In Eq. 1, the passive component is linearly viscoelastic with a viscous coefficient μ_P.

The model also requires the equilibration rate $r(L)$ and isometric tension $T_{M0}(L)$ as functions of L. We assume that both functions are generated from a length-dependent myosin-actin affinity $K(L)$ that expresses an appropriate model of stretch activation. The simplest approximation is to set

$$r(L) = (K(L) + 1)g, \; T_{M0}(L) = \frac{K(L)}{K(L) + 1}T_{00} \quad (4)$$

in terms of a constant actomyosin dissociation rate g and a binding rate $K(L)g$. Thus, T_{00} is maximally activated myosin tension at full overlap, which can be associated with a fiber, unit cross-sectional area of fiber or a single myosin filament. To avoid these choices, tension is measured in units of T_{00}.

Our preferred model of stretch activation involves a radial compressive force generated by titin-actin linkages near the Z-line (Fig. 2 *C*), as observed in skinned fibers (15). It leads to a lattice spacing that decreases linearly with sarcomere length, and hence a length-dependent actomyosin affinity of the form

$$K(L) = K_*\exp\left(-\Delta(L - L_*)^2/2\right), \quad (5)$$

for $L < L_*$ (legend to Fig. 2). To be specific, let $K(L) = K_*$ when $L > L_*$. The coefficient Δ can be expressed in terms of the bending stiffness of the S2 rod connecting dimeric myosin to the thick filament, and the slope of the lattice spacing as a function of sarcomere length, as described in the figure legend. In an intact fiber, the average lattice spacing must also decrease with sarcomere length to maintain constant volume.

The single-sarcomere model is completely defined by Eqs. 1–5 and a boundary condition for the effect of an external load. The most general boundary condition is auxotonic, with a damped elastic load. Then

$$T(t) = F - \kappa_S L(t) - \mu_S v(t), \quad (6)$$

where F is the load supplied at zero sarcomere length. This load could be generated elastically by setting the resting length of the elastic element, or it could be supplied independently (Fig. 2 *D*). In the latter case, isotonic conditions are recovered when $\kappa_S = \mu_S = 0$.

Equations 1 and 6 combine to yield a single equation for $L(t)$, namely

$$\dot{L}(t) \equiv v(t) = \frac{F - \rho T_M(L) - T_P(L) - \kappa_S L}{\mu_S + \mu_P T_P(L)}, \quad (7)$$

and Eqs. 2 and 7 are a closed pair of coupled first-order differential equations for the dynamical behavior of the model. Equation 7 shows that the viscous component of passive tension is essential to give a finite velocity response in the isotonic case.

Predictions

Numerical studies of the single-sarcomere model confirm that SPOC is a rare phenomenon. In most cases, an isotonic sarcomere at partial overlap of filaments is either stable, or it moves rapidly to near zero overlap or the ascending limb, depending on the direction of the original displacement from the fixed point. However, the model does generate length oscillations for a range of activation levels defined by myosin-actin affinity K_2 at full filament overlap (2.6 μm), with realistic values for the stretch activation coefficient Δ and the parameters T_{P0}, ξ, μ_P of passive tension. We present some examples and then the results of a method for locating SPOC behavior in parameter-space.

Examples for fast and slow fibers

Fig. 4 *A* shows an example of spontaneous oscillations in sarcomere length from the single-sarcomere model under isotonic conditions, starting from a sarcomere length of 2.7 μm on the descending limb. The parameter values have been chosen to simulate a slow-twitch fiber such as rat/mouse soleus at 20°C, and are listed in Table 1. Note especially the low value of g (0.2 s). Steady oscillations develop after one cycle, and are maintained indefinitely with a period of 10.7 s. The waveform is asymmetric, where most of the lengthening phase is faster than the shortening phase. However, the initial lengthening is slower when the sarcomere has been driven into full overlap ($L < 2.6$ μm), because the descending limb is not present to accelerate lengthening. Oscillations of equal amplitude and opposite phases are present in active and passive tension, so that their sum is constant.

For a fast fiber, the myosin detachment rate g was increased by a factor of four, and α (the slope of the normalized tension-velocity curve for shortening) was reduced from 1.5 μm^{-1} to 0.3 μm^{-1} to raise contractile tension in shortening. A threefold increase in unloaded shortening velocity was imposed by changing the value of β_-. Oscillations ensued (Fig. 4 *B*) without changing any other parameter values, with a period of 4.4 s after the growth phase.

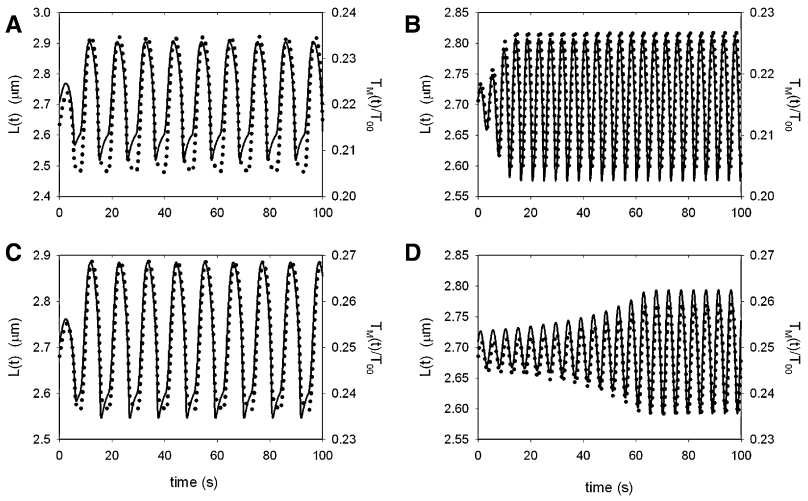

FIGURE 4 SPOC waveforms for sarcomere length $L(t)$ (*solid line*) and scaled myosin tension $T_M(t)$ (*points*) from the single-sarcomere model with the parameter values of Table 1. (*A*) Slow fiber, isotonic load. (*B*) Fast fiber, isotonic load. (*C*) Slow fiber, auxotonic load with $\kappa_S/T_{00} = 0.01\ \mu m^{-1}$, $\mu_S/\kappa_S = 0.5\ s^{-1}$. (*D*) Fast fiber, same auxotonic load. All waveforms start from the fixed point at 2.7 μm, perturbed by an initial length change of 0.01 μm.

For an auxotonic load, the conditions for SPOC are more restrictive as there is an extra restoring force to limit oscillations in sarcomere length. There is an upper limit to the stiffness of the load for which the single-sarcomere model develops oscillations. The examples shown in Fig. 4, *C* and *D*, were generated with $\kappa_S/T_{00} = 0.01\ \mu m^{-1}$ and $\mu_S/T_{00} = 0.005$ s/μm. To get oscillations, it was necessary to increase the value of K_2 from 0.25 to 0.30. The periods of oscillation (11.0 s and 4.7 s for the fast and slow fiber models) are very similar to the isotonic values, but for the fast fiber the growth rate in this example is very slow.

TABLE 1 Model parameters for slow and fast fibers

Parameter	Slow fiber	Fast fiber
L_0 (μm)	2.7	2.7
L_1 (μm)	2.4	2.4
L_2 (μm)	2.6	2.6
L_3 (μm)	4.0	4.0
L_* (μm)	3.6	3.6
K_2	0.25 (0.3)	0.25 (0.3)
G (s^{-1})	0.20	0.80
Δ (μm^{-2})	1.0	1.0
α (μm^{-1})	1.5	0.30
β_- (μm^{-1})	1.3	0.23
β_+ (μm^{-1})	1.5	0.30
T_{P0}/T_{00}	1.0	1.0
ξ (μm^{-1})	3.0	3.0
μ_P (s/μm)	1.25	1.25
κ_S/T_{00} (μm^{-1})	0 (0.01)	0 (0.01)
μ_S/T_{00} (s/μm)	0 (0.005)	0 (0.005)

Parameters are nominally for rat soleus and rat EDL at 20°C, which generated the SPOC waveforms shown in Fig. 4. The value of the stretch-activation coefficient Δ corresponds to $\kappa_{rod} = 0.11$ pN/nm for the bending stiffness of the myosin-S2 rod and $\gamma = 0.006$ (15). A much smaller value of κ_{rod} in solution (28) suggests that myosin-S2 is much stiffer in the electrostatic environment of the sarcomere. As described in the main text, the values of α and β_- correspond to values of 0.14 (slow) and 0.28 (fast) for the Hill parameter a/T_0, and to unloaded contraction velocities of 5.0 μm/s (slow) and 14.3 μm/s (fast) per sarcomere (29). Choosing $\beta_+ = \alpha$ gives a steady contractile tension of $2T_0$ at large stretch velocities. Observed values of ξ range from 6 to 2 μm^{-1} (3,23,30), and the value of μ_P is similar to that suggested by Denoth et al. (32). The entries are primarily for isotonic SPOC. Entries in parentheses indicate the changes made for SPOC under auxotonic conditions.

Although these examples show that the model can generate spontaneous oscillatory contractions, the values of all parameters have been carefully chosen to fit experimental data or to illustrate the model. These examples do not show the sensitivity of the model, in particular variations in the period of oscillation, growth rate, and waveform, to changes in parameter values, which are considered in the next subsection. Finally, in the concluding discussion we consider the relevance of the single-sarcomere model to SPOC as observed in real muscle fibers or myofibrils.

Phase diagrams for SPOC

To locate the values of model parameters that give SPOC behavior, it is essential to use a stability analysis of the fixed-point on the descending limb, as in Appendix SA in the Supporting Material. Here we summarize the results of this analysis in terms of phase diagrams in parameter space, referring to the functions A, B, and D where A and B are the trace and determinant of the stability matrix and $D = 4B - A^2$. The fixed point is stable when $A < 0$ and $B > 0$, which in practice occurs at very low activation and corresponds to relaxed muscle. When the fixed point is unstable, SPOC is expected when $A > 0$ and $D > 0$; otherwise, the sarcomere pops to the stable fixed point at longer lengths or on the ascending limb. Our results confirm that SPOC occurs in a narrow domain of parameter values.

The boundaries between the relaxed, popped, and SPOC phases have been calculated as a function of model parameters for auxotonic conditions. The model contains 16 parameters, of which four (L_1, L_2, L_3, L_*) are treated as fixed structural parameters of the muscle (Table 1). Of the remainder, β_+ and β_- are eliminated by linearization about the fixed point, and it turns out that the effects of α and g are approximately described by their product $\eta = \alpha g$. The remaining eight parameters are F, K_*, Δ (the stretch-activation

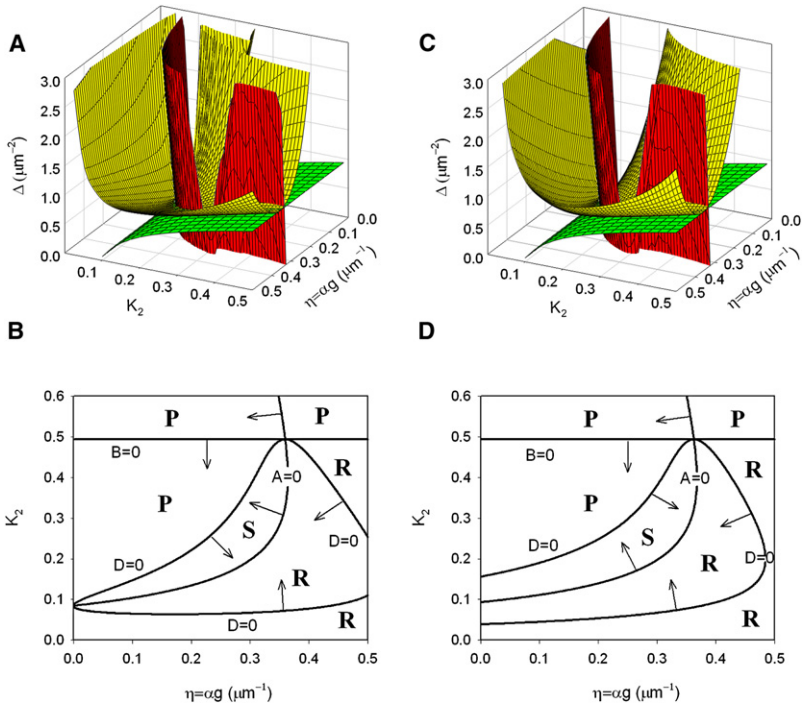

FIGURE 5 Phase diagrams for the isotonic sarcomere, showing the relaxed, popped, and SPOC phases (R, P, S) and their boundaries as functions of selected model parameters. The values of constant parameters are for the slow fiber in Table 1. (A) The phases in (η, K_2, Δ) space where $\eta = \alpha g$ is varied at constant α. The dark (red online), intermediate (green online), and light (yellow online) surfaces are the phase boundaries $A = 0$, $B = 0$, or $D = 0$ respectively, as defined in Appendix SA. SPOC lies between the left-hand branches of the dark (red online) and light (yellow online) surfaces above their line of intersection, which define a minimum value of Δ. (B) A horizontal slice of the previous graph at $\Delta = 1.0\ \mu m^{-2}$, showing the dependence on η and K_2. The arrows define regions where A, B, or $D > 0$. (C) Phases in (η, K_2, Δ) space where $\eta = \alpha g$ is varied at constant g. (D) Intersections of the above plot with the plane $\Delta = 1.0\ \mu m^{-2}$.

coefficient), the passive tension parameters T_{P0}/T_{00}, ξ, μ_P and the load parameters κ_S, μ_S. F is related to the sarcomere length L_0 of the fixed point by the equation $F = T_0(L_0) + \kappa_S L_0$ where $T_0(L) = \rho(L)T_{M0}(L) + T_P(L)$. Calculations were made only for the fixed point on the descending limb ($L_2 < L_0 < L_3$), and were organized as follows, using the parameter values of Table 1 as a control. Items 1–6 apply to isotonic SPOC, where $\kappa_S = \mu_S = 0$.

1. Phase boundaries were first calculated as surfaces in the space (η, K_2, Δ) of the three key parameters, which determine the response rate, actin-myosin affinity, and the strength of stretch activation, respectively. Here $K_2 = K(L_2)$, the affinity at the longer end of the region of full overlap (Fig. 2 B); the quantity K_* follows from Eq. 5. These surfaces are shown in Fig. 5 A, and show that a minimum amount of stretch activation ($\Delta > 0.64\ \mu m^{-2}$) is required for SPOC. A clearer picture emerges if solutions are calculated in a horizontal plane. Fig. 5 B shows the phase boundary lines as a function of η and K_2 for a slightly higher value of Δ. The lines $A = 0$ and $D = 0$ are both re-entrant, as expected from Fig. 5 A, and the region $A > 0$, $D > 0$, which generates the SPOC phase, puts global minimum and maximum values of 0.09 and 0.50 on K_2, and a global maximum of 0.35 on η. However, for $\eta < 0.35$ the minimum and maximum values of K_2 lie closer together. Thus, SPOC is a phenomenon confined to a narrow range of low activation levels. Furthermore, the restriction on η suggests that SPOC is favored for slow-twitch muscles where the phase-4 rate g is under 1 s^{-1} (25).
2. Fig. 5 B also shows that the slope of the tension-length curve $T_0(L)$, which determines the sign of B, is not a determinant of SPOC. Both the SPOC and relaxed phases occur when $B > 0$, where the slope of the tension-length curve is positive. Moreover, the transition from negative to positive values of B as K_2 is lowered does not necessarily correspond to a phase transition; for $\eta < 0.34$ the boundary $B = 0$ merely signals popping from an unstable node rather than popping from a saddle point, whereas for $\eta > 0.34$ this boundary marks the division between the popped and relaxed phases. Equally, the transition from negative to positive values of D can mark the difference between two kinds of relaxed phase, stemming from a stable spiral or a stable node, whereas for $\eta < 0.34$ the upper branch of the line $D = 0$ separates the popped and SPOC phases. In practice, these different kinds of a single phase may not be observable.
3. The values of $\eta = \alpha g$ in Fig. 5, A and B, were generated with a fixed value of α, as in Table 1. Those in Fig. 5, C and D, were generated with a fixed value of g, again as in the table. They are similar in character, but at low values of η the range of activation levels for SPOC is less constrained when caused by a low value of α (Fig. 5 D) than by a low value of g (Fig. 5 B).
4. The effects of changing the initial sarcomere length L_0 were calculated in terms of phase boundary lines in the (L_0,K_2) plane. Fig. 6 A shows that the SPOC phase is confined to sarcomere lengths near full overlap, with the widest range of activation levels occurring when L_0 just exceeds $L_2 = 2.6\ \mu m$. The maximum initial length for SPOC was 2.87 μm. Although stretch activation is stronger at this length, this phase boundary cannot be extended by changing the parameters of passive tension.

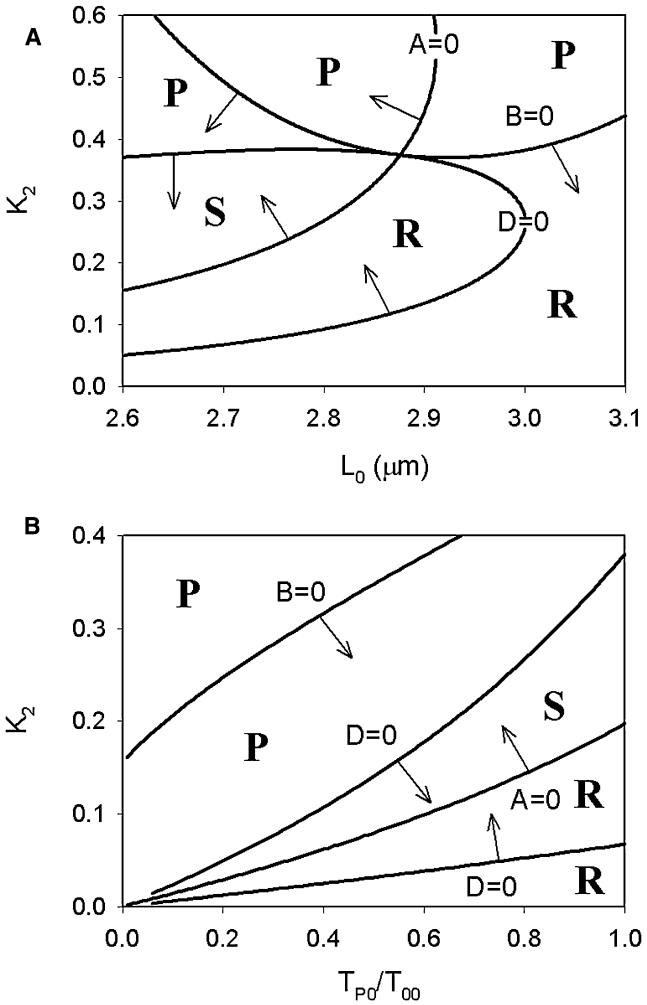

FIGURE 6 (*A*) The phases as a function of affinity K_2 and the sarcomere length L_0 at the fixed point. (*B*) Similarly, showing the dependence on the strength of passive tension T_{P0} relative to maximum active tension T_{00} on the plateau. Control values and labels for phases and their boundaries are defined in Fig. 5.

5. Phase boundaries as a function of the strength of passive tension and myosin affinity are shown in Fig. 6 *B*. Again, there are minimum and maximum values of affinity for a given value of T_{P0}/T_{00}, with the largest range achieved when $T_{P0}/T_{00} > 1.0$. The plot was not continued to higher values because they are generally not found in unfatigued muscle. The coefficient μ_P determines the ratio of viscous to elastic responses in passive tension, and was set at 3.0 s/μm throughout (31).
6. The occurrence of SPOC and the shape of its waveform are not sensitive to the parameters $\beta_\pm$ that control the shape of the tension-velocity curve at large velocities, either in shortening or lengthening. This is confirmed by the waveforms in Fig. 4, which show that the maximum speed of length change is under 0.5 μm/s, an order of magnitude below the unloaded shortening velocities of 5 μm/s and 15 μm/s.

When the SPOC phase in parameter space has been located, it is of interest to calculate the growth rate $A/2$ and the initial frequency (in radians/s) of oscillation $(D/4)^{1/2}$ (see Appendix SA) as a function of selected parameters. As a function of L_0, the growth rate and frequency are fastest when $L_0 \geq L_2$, near full overlap (Fig. 7). As a function of K_2, the growth rate is zero and the oscillation frequency is a maximum at the minimum value of K_2 for the SPOC domain in Fig. 5, *B* and *D*, where $A = 0$. Conversely, the growth rate is a maximum and the oscillation frequency is zero at the maximum value of K_2 for SPOC, where $D = 0$. Thus the fastest oscillations are expected at the lowest level of activation in the SPOC range and near full filament overlap, whereas there seems to be no lower limit to the frequency.

For auxotonic SPOC, there is a global maximum stiffness to the elastic element of the load. For example, $\kappa_S/T_{00} < 0.032\ \mu m^{-1}$ in Fig. 8 *A*, where the corresponding damping constant μ_S was set by choosing $\mu_S/\kappa_S = 0.5\ s^{-1}$. The phase boundaries are relatively insensitive to the value of this ratio.

DISCUSSION

Under isotonic conditions, the single-sarcomere model, in which all sarcomeres are assumed to oscillate in phase, predicts spontaneous oscillations essentially as observed by

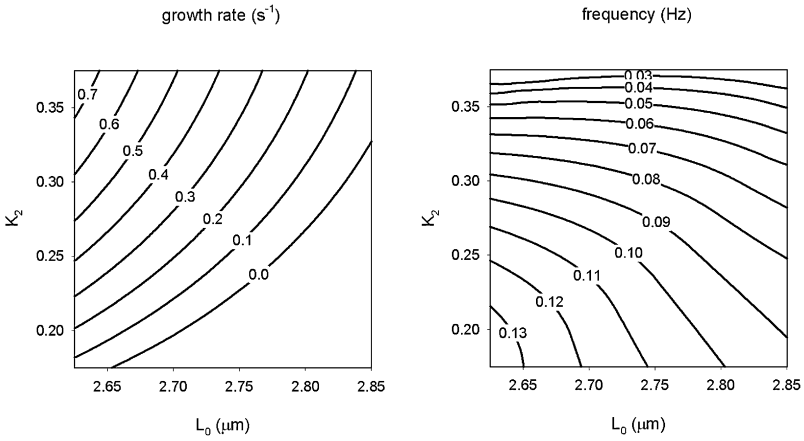

FIGURE 7 Contour plots for the growth rate (*A*) and frequency (*B*) of length oscillations of the isotonic slow fiber, as a function of myosin affinity K_2 at length L_2 and sarcomere length L_0 at the fixed point. In *A*, the region below the zero-rate contour is the relaxed phase. In *B*, the frequency of oscillation falls to zero as K_2 increases to the S-P boundary line shown in Fig. 6 *A*. Control values are for the slow fiber of Table 1.

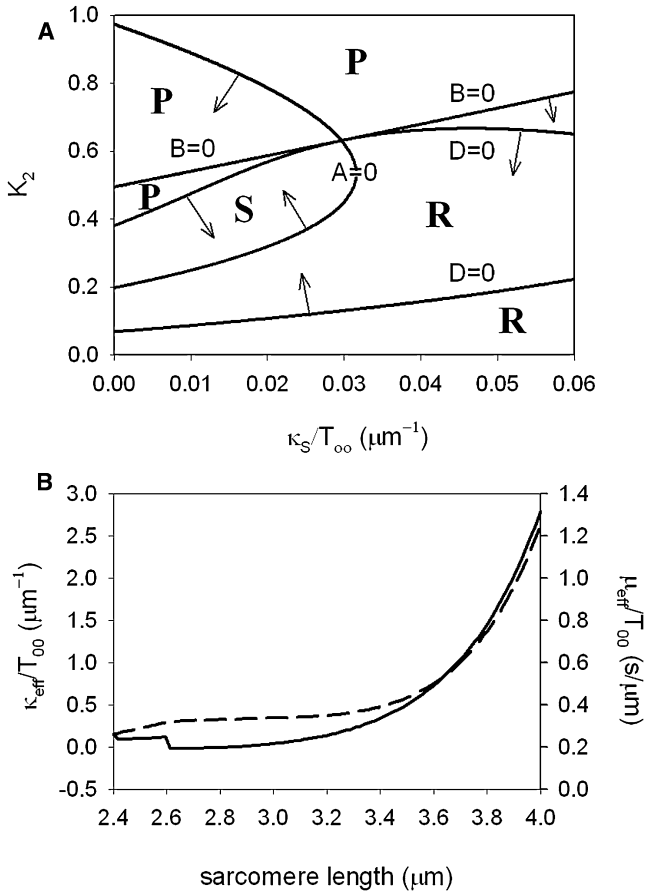

FIGURE 8 (*A*) The phase boundary for auxotonic SPOC as a function of normalized load stiffness κ_S/T_{00} for the slow fiber of Table 1. The damping constant μ_S of the load was varied in proportion to κ_S. (*B*) The effective stiffness κ_{eff} and damping constant μ_{eff} of a single sarcomere for slow length changes, calculated from Eqs. B3 in Appendix SB for the slow-fiber parameters of Table 1. At full activation ($K_2 >> 1$), κ_{eff} is much larger, for example 20 nN/μm per myofilament on the plateau of the tension-length curve if $T_{00} = 0.4$ nN per myofilament. The instantaneous stiffness of active muscle (58 nN/μm per myofilament for rabbit psoas muscle (33) is larger again. At large sarcomere lengths, κ_{eff} is dominated by passive tension and $\mu_{eff}/\kappa_{eff} \approx 0.5\ s^{-1}$ as in Table 1.

Yasuda et al. (21) for a skeletal myofibril, where all sarcomeres oscillate in phase. The observed cycle of length oscillation has a period of 2.0–2.6 s for different force levels, with a rapid rise in length followed by a slow fall. The predicted waveform for a fast fiber (Fig. 5 *B*) has a similar period but differs in shape; the rise rate is not so fast, probably because the actin-myosin kinetics of the model have been simplified. SPOC is observed at different force levels under conditions where the average length increases with force, but the filaments remain in partial overlap, similar to the lower tension-length curve on the descending limb in Fig. 3 *A*. Passive tension is present but falls to very small values at the minimum length of the cycle (Fig. 3 *A*), also as observed (3).

Under auxotonic conditions, the single-sarcomere model predicts a maximum load stiffness for the occurrence of SPOC. Here the model can be tested against the myofibril experiment of Anazawa et al. (24), with 36 sarcomeres and a microneedle load with $\kappa_S = 10$ nN/μm, $\mu_S = 0.33$ nN $\times$ s/μm. If there were just one sarcomere, the equivalent normalized stiffness κ_S/T_{00} would be 0.36 μm^{-1} after multiplying by 36 and dividing by isometric tension at full activation (say 1000 nN for a bundle of diameter 3 μm). Thus the model fails this test; the above value of κ_S/T_{00} is an order of magnitude above the predicted upper limit of 0.032 μm^{-1}. To sharpen the paradox, note that SPOC is also observed in fixed-end fibers, where the stiffness of the load is set by the tension transducer (typically 10^5 nN/μm). For a fiber of diameter 50 μm, $T_{00} \sim 4 \times 10^5$ nN, so $\kappa_S/T_{00} \approx 200\ \mu m^{-1}$ for a 2 mm fiber with 800 sarcomeres, which is four orders of magnitude above the upper limit. In the sense of the model, neither experiment is weakly auxotonic.

Why is SPOC observed experimentally when the stiffness of the load exceeds the upper limit predicted by the model? The answer is that SPOC is a multisarcomeric phenomenon; each sarcomere moves in response to an equivalent auxotonic load consisting of all other sarcomers acting in series with themselves and with the external load. Although all sarcomeres ultimately oscillate, the single-sarcomere model can be applied if the other sarcomeres can be represented by passive mechanical elements, here taken to be a spring and dashpot in parallel. Estimates for the equivalent stiffness κ_S and damping constant μ_S of the fiber can be made from the single-sarcomere model, using formulae derived in Appendix SB and graphed in Fig. 8 *B*. The figure shows that the average value of κ_S/T_{00} per sarcomere over the range of length-oscillation in Fig. 4 *A* is $<0.2\ \mu m^{-1}$. For 36 sarcomeres in series, the equivalent normalized stiffness is 0.0056 μm^{-1}, which is less than the maximum value of 0.032 μm^{-1} predicted for a slow fiber by a comfortable margin, even for a fixed-end fiber. Similar estimates apply if the rest of the fiber has not started to oscillate. The value of μ_S was set at $0.5\kappa_S$, which is correct at longer lengths (Fig. 8 *B*).

When viewed in this light, the difference between nearly isotonic and fixed-end boundary conditions for the whole fiber appear to be less important, and attention should instead be focused on any initial inhomogeneity of the sarcomeres, and how a wavefront is able to propagate. These matters are properly addressed by a multisarcomeric model with a suitable interaction between adjacent sarcomeres, which might also explain why the single-sarcomere model does not generate tension oscillations of sufficient amplitude under auxotonic conditions. Note also that the predicted length-oscillation waveforms in Fig. 4 do not show the rapid lengthening that is sometimes observed (4,19); this deficiency is related to actomyosin kinetics (27) and is a result of restricting transient myotension responses to the slowest component in Eq. 2. In practice, rapid lengthening is expected when the load F exceeds the maximum steady-state tension $(1 + \alpha/\beta_+)T_0(L)$ for lengthening, which could occur near the minimum length of the SPOC cycle.

The power of the model is best shown by its ability to predict known conditions for the existence of SPOC. The predicted phase diagrams in Fig. 5 agree with observations that limit SPOC to a low-[Ca^{2+}] domain (2,5), which is specified in the model by a range of myosin affinities K_2. The ratio of SPOC frequencies observed in slow and fast fibers was 0.19 (31), which compares well with the predicted dependence of the SPOC frequency on g in Fig. 8, where the ratio between the g values for slow and fast fibers is 0.25 (Table 1). Furthermore, an increase in temperature from 22 to 35°C increased the frequency of SPOC in slow fibers three- to fivefold (2), in line with the increased myofibrillar ATPase. A decrease in temperature from 22 to 5°C reduced active tension by a factor of three (2), which raises the ratio of passive to active tension by the same factor and leads to the abolition of SPOC as predicted in Fig. 6 *B*. Conversely, a reduction in the passive component by detergent treatment produces a reduction in the SPOC frequency (31), which is predicted by Fig. 6 *B*.

Ishiwata et al. (12) have also measured a phase diagram for the contractile, relaxed, and SPOC phases as a function of Pi and ADP levels in the absence of calcium. Their findings are summarized as follows: the contractile phase occurs at ADP levels above a threshold value and can be converted to the SPOC phase by adding Pi or removing ADP, whereas relaxed behavior is always found at subcritical levels of ADP. These findings agree with the phase diagram in Fig. 5 *B* if K_2 is a decreasing function of [Pi] and g is a decreasing function of [ADP]. Starting from the lower-left part of the popped (contractile) phase in Fig. 5 *B*, the corresponding maneuvers are to decrease K_2 or increase $\eta = \alpha g$, both of which lead to the SPOC phase. A further increase in αg leads to the relaxed phase. However, the relaxed phase is replaced by the popped phase when K_2 is increased above 0.5. Such high values of K_2 may not be reached by reducing the phosphate concentration, which has a logarithmic effect on actomyosin affinity and isometric tension. Note that added Pi can also convert the SPOC phase to the relaxed phase in bovine cardiac muscle (13).

CONCLUSIONS

We conclude that in skeletal muscle, SPOC is indeed a separate phase of the muscle in the presence of ATP, confined to sarcomere lengths on the descending limb with partial filament overlap (3,5). In terms of levels of activation, SPOC lies between the relaxed phase at very low activation ($K_2 << 1$), and the popped phase at high activation ($K_2 > 1$) where sarcomeres on the descending limb have moved either toward zero overlap or the ascending limb. At intermediate levels, the inherent instability of a fixed point on the descending limb can be converted from popping to SPOC behavior by a stretch-activation mechanism, which cures the instability after the time delay required for heads to detach and rebind. Viscoelastic passive tension is generally required to make lengthening sarcomeres turn around and start the shortening phase of a cycle of oscillation.

Our single-sarcomere model recognizes that SPOC is solely a property of the contractile apparatus, namely actin filaments in interaction with myosin heads that hydrolyze ATP. Thus the effects of the regulatory system, which under physiological conditions limit SPOC to a range of low [Ca^{2+}] levels, can be described solely in terms of their effects on actin-myosin affinity, as long as that affinity is boosted at longer lengths by a stretch-activation mechanism within the contractile system. This remarkable conclusion is supported by the three examples of regulatory decoupling given in the introduction. The model also predicts the occurrence of SPOC as a function of added Pi and ADP (12) by decreasing K_2 and g respectively, and should be capable of describing the effects of other manipulations of contractile conditions. The development of a true multisarcomeric model will be the subject of further study.

SUPPORTING MATERIAL

Two appendices and five equations are available at http://www.biophysj.org/biophysj/supplemental/S0006-3495(09)00555-4.

This work was supported by ARC and National Health Medical Research Council grants to D.G.S.

REFERENCES

1. Fabiato, A., and F. Fabiato. 1978. Myofilament-generated tension oscillations during partial calcium activation and activation dependence of the sarcomere length-tension relation of skinned cardiac cells. *J. Gen. Physiol.* 72:667–699.
2. Stephenson, D. G., and D. A. Williams. 1981. Calcium-activated force responses in fast-and slow-twitch skinned muscle fibers of the rat at different temperatures. *J. Physiol.* 317:281–302.
3. Stephenson, D. G., and D. A. Williams. 1982. Effects of sarcomere length on the force-pCa relation in fast-and slow-twitch skinned muscle fibers from the rat. *J. Physiol.* 333:637–653.
4. Okamura, N., and S. Ishiwata. 1988. Spontaneous oscillatory contraction of sarcomeres in skeletal myofibrils. *J. Muscle Res. Cell Motil.* 9:111–119.
5. Shimamoto, Y., M. Suzuki, and S. Ishiwata. 2008. Length-dependent activation and auto-oscillation in skeletal myofibrils at partial activation by Ca^{2+}. *Biochem. Biophys. Res. Commun.* 366:233–238.
6. Gordon, A. M., A. F. Huxley, and F. J. Julian. 1966. The variation in isometric tension with sarcomere length in vertebrate muscle fibers. *J. Physiol.* 184:170–192.
7. Ford, L. E., A. F. Huxley, and R. M. Simmons. 1981. The relation between stiffness and filament overlap in stimulated frog muscle fibers. *J. Physiol.* 311:218–249.
8. Endo, M. 1972. Stretch-induced increase in activation of skinned muscle fibers by calcium. *Nat. New Biol.* 237:211–213.
9. Smith, D. A., and D. G. Stephenson. 1994. Theory and observation of spontaneous oscillatory contractions in skeletal myofibrils. *J. Muscle Res. Cell Motil.* 15:369–389.
10. Geeves, M. A., and S. S. Lehrer. 1994. Dynamics of the muscle thin filament regulatory switch: the size of the cooperative unit. *Biophys. J.* 67:273–282.
11. Johnson, J. D., D. E. Robinson, S. J. Robertson, A. Schwarz, and J. D. Potter. 1981. Ca^{2+} exchange with troponin and the regulation of

muscle contraction. *In* The Regulation of Muscle Contraction: Excitation-Contraction Coupling. A. Grinnell and M. A. B. Brazier, editors. Academy Press, New York. 241–259.

12. Ishiwata, S., T. Anazawa, T. Fujita, N. Fukuda, H. Shimizu, et al. 1993. Spontaneous tension oscillation (SPOC) of muscle fibers and myofibrils: minimum requirements for SPOC. *In* Mechanism of Myofilament Sliding in Muscle Contraction. H. Sugi and G. H. Pollack, editors. Plenum, New York. 545–556.
13. Fukuda, N., H. Fujita, T. Fujita, and S. Ishiwata. 1996. Spontaneous tension oscillation in skinned bovine cardiac muscle. *Pflugers Arch.* 433:1–8.
14. Fujita, H., and S. Ishiwata. 1998. Spontaneous oscillatory contraction without regulatory proteins in actin filament-reconstituted fibers. *Biophys. J.* 75:1439–1445.
15. Cazorla, O., Y. Wu, T. C. Irving, and H. Granzier. 2001. Titin-based modulation of calcium sensitivity of active tension in mouse skinned cardiac myocytes. *Circ. Res.* 88:1028–1035.
16. Knupp, C., P. K. Luther, and J. M. Squire. 2002. Titin organisation and the 3D architecture of the vertebrate-striated muscle I-band. *J. Mol. Biol.* 322:731–739.
17. Matsubara, I., Y. E. Goldman, and R. M. Simmons. 1984. Changes in the lateral filament spacing of skinned muscle fibers when cross-bridges attach. *J. Mol. Biol.* 173:15–33.
18. Shimamoto, Y., F. Kono, M. Suzuki, and S. Ishiwata. 2007. Nonlinear force-length relationship in the ADP-induced contraction of skeletal myofibrils. *Biophys. J.* 93:4330–4341.
19. Tskhovrebova, L., J. Trinick, J. A. Sleep, and R. M. Simmons. 1997. Elasticity and unfolding of single molecules of the giant muscle protein titin. *Nature.* 387:308–312.
20. Kellermayer, M. S. Z., S. B. Smith, H. L. Granzier, and C. Bustamente. 1997. Folding-unfolding transitions in single titin molecules characterized with laser tweezers. *Science.* 276:1112–1116.
21. Yasuda, K., Y. Shindo, and S. Ishiwata. 1996. Synchronous behavior of spontaneous oscillations of sarcomeres in skeletal myofibrils under isotonic conditions. *Biophys. J.* 70:1823–1829.
22. Morgan, D. L. 1990. New insights into the behavior of muscle during lengthening. *Biophys. J.* 57:209–221.
23. Edman, K. A. P. 1979. The velocity of unloaded shortening and its relation to sarcomere length and isometric force in vertebrate muscle fibers. *J. Physiol.* 291:143–159.
24. Anazawa, T., K. Yasuda, and S. Ishiwata. 1992. Spontaneous oscillation of tension and sarcomere length in skeletal myofibrils. *Biophys. J.* 61:1099–1108.
25. Burton, K., R. M. Simmons, J. Sleep, R. M. Simmons, K. Burton, et al. 2006. Kinetics of force recovery following length changes in active skinned fibers from rabbit psoas muscle: analysis and modeling of the late recovery phase. *J. Physiol.* 573:305–328.
26. Hill, A. V. 1938. The heat of shortening and the dynamic constants of muscle. *Proc. R. Soc. Lond., B, Biol. Sci.* 126:136–195.
27. Harry, J. D., A. W. Ward, N. C. Heglund, D. L. Morgan, and T. A. McMahon. 1990. Crossbridge cycling theories cannot explain high-speed lengthening behavior in frog muscle. *Biophys. J.* 57:201–208.
28. Adamovich, I., S. M. Mijailovich, and M. Karplus. 2008. The elastic properties of the structurally characterized myosin II S2 subdomain: a molecular dynamics and normal mode analysis. *Biophys. J.* 94:3779–3789.
29. Ranatunga, K. W. 1982. Temperature dependence of shortening velocity and rate of isometric tension development in rat skeletal muscle. *J. Physiol.* 329:465–483.
30. Altringham, J. D., and R. Bottinelli. 1985. The descending limb of the sarcomere length-force relation in single muscle fibers of the frog. *J. Muscle Res. Cell Motil.* 6:585–600.
31. Fink, R. H. A., D. G. Stephenson, and D. A. Williams. 1986. Potassium and ionic strength effects the isometric force of skinned twitch muscle fibers of the rat and toad. *J. Physiol.* 370:317–337.
32. Denoth, J., E. Stussi, G. Csucs, and G. Danuser. 2002. Single muscle fiber contraction is dictated by inter-sarcomere dynamics. *J. Theor. Biol.* 216:101–122.
33. Linari, M., M. Caremani, C. Piperio, P. Brandt, and V. Lombardi. 2007. Stiffness and fraction of myosin motors responsible for active force in permeabilized muscle fibers from rabbit psoas. *Biophys. J.* 92:2476–2490.
34. Nicolis, G., and I. Prigogine. 1977. Self-Organization in Nonequilibrium Systems. Wiley-InterScience, New York. 76–89.